Engineering of TiO_2 Anode toward a Record High Initial Coulombic Efficiency Enabling High-Performance Low-Temperature Na-ion Hybrid Capacitors

Meiling Kang,[a, b] Yingying Wu,[a] Xin Huang,[a] Kaiqiang Zhou,[a, b] Zhigao Huang[a, b] and Zhengsheng Hong*[, a, b]

[a]Fujian Provincial Key Laboratory of Quantum Manipulation and New Energy Materials, College of Physics and Energy, Fujian Normal University, Fuzhou, Fujian 350117, China.

[b]Fujian Provincial Collaborative Innovation Center for Optoelectronic Semiconductors and Efficient Devices, Xiamen, 361005, China

*Corresponding Authors: E-mail: winter0514@163.com

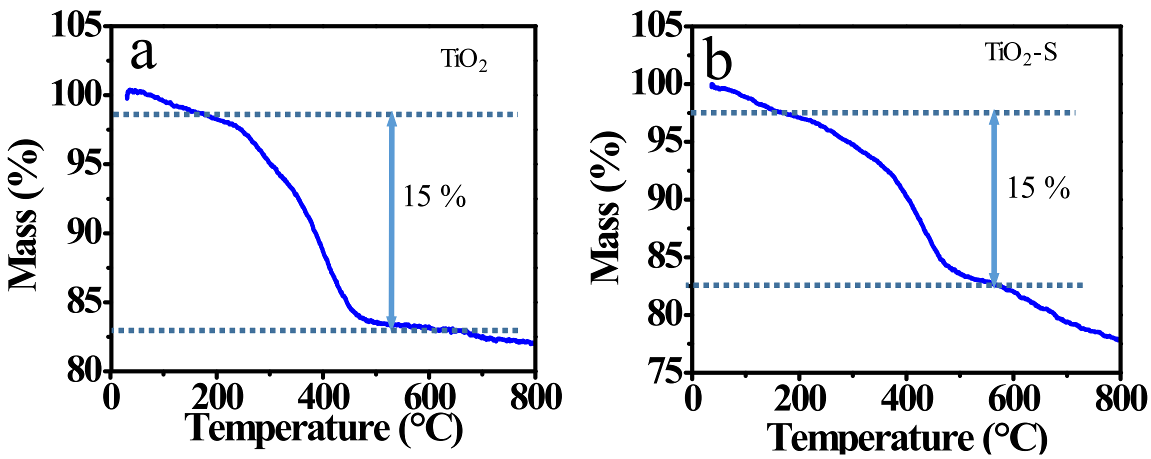

Fig. S1. TG curves of TiO_2 (a) and TiO_2-S (b).

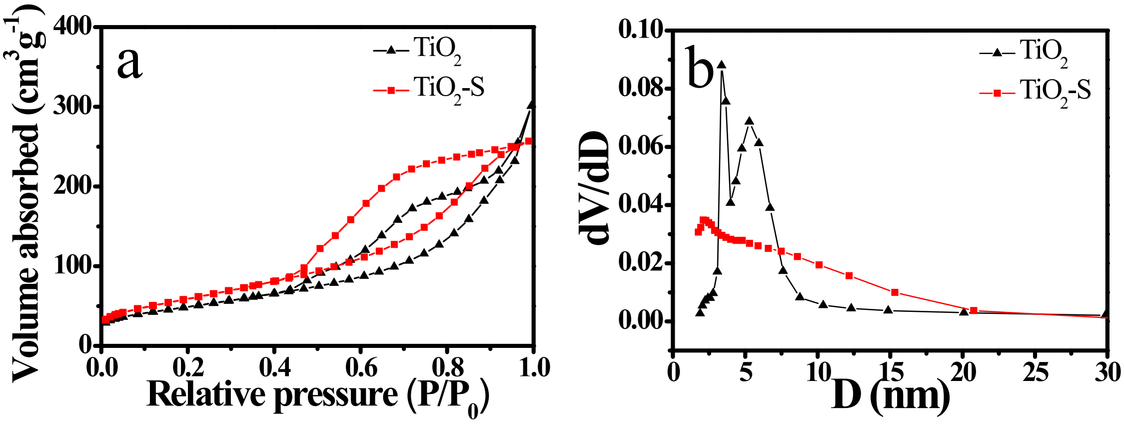

Fig. S2. (a) Nitrogen adsorption-desorption curves of TiO_2 and TiO_2-S, (b) the corresponding BJH pore size distribution.

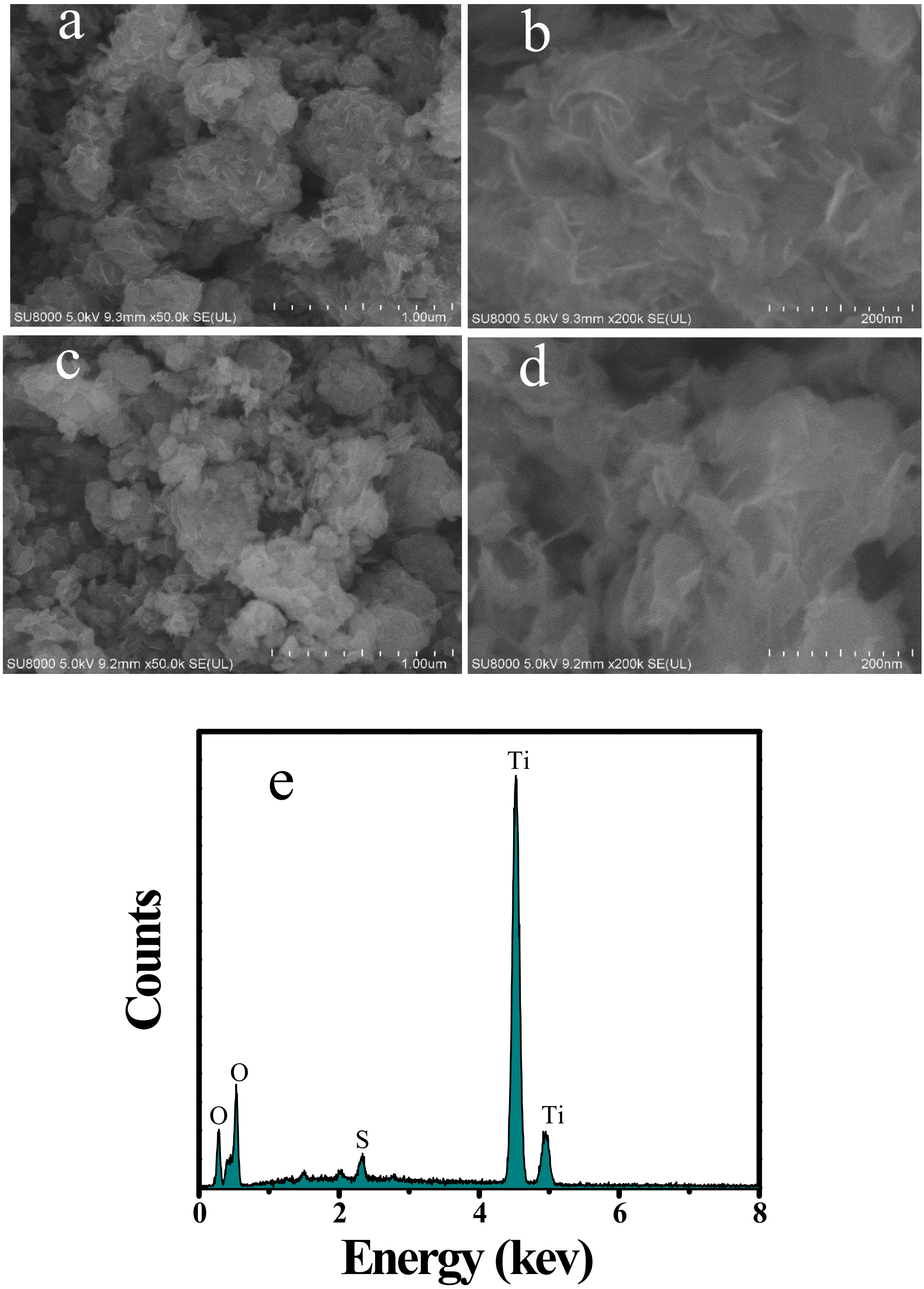

Fig. S3. SEM images of (a, b) the as-made product, (c, d) TiO_2. (e) EDS pattern of TiO_2-S.

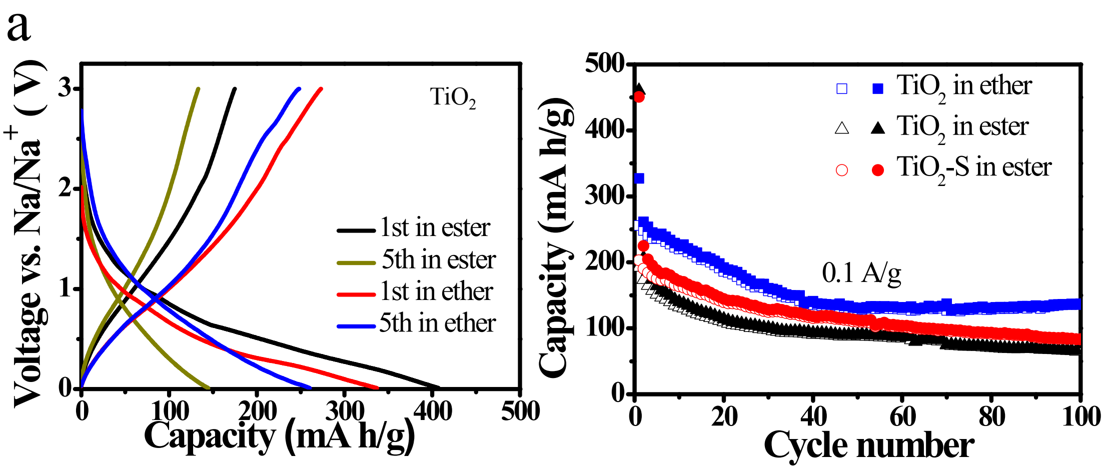

Fig. S4. a) Charge-discharge profiles for TiO_2 in ether and ester under 0.05 A/g. b) Cycling stability of the different electrodes in different electrolytes.

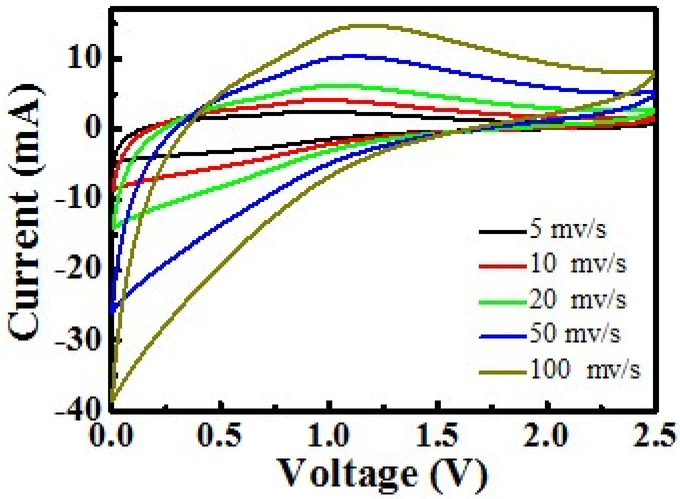

Fig. S5. CV curves of TiO_2-S electrode in ether electrolyte under high sweep rates.

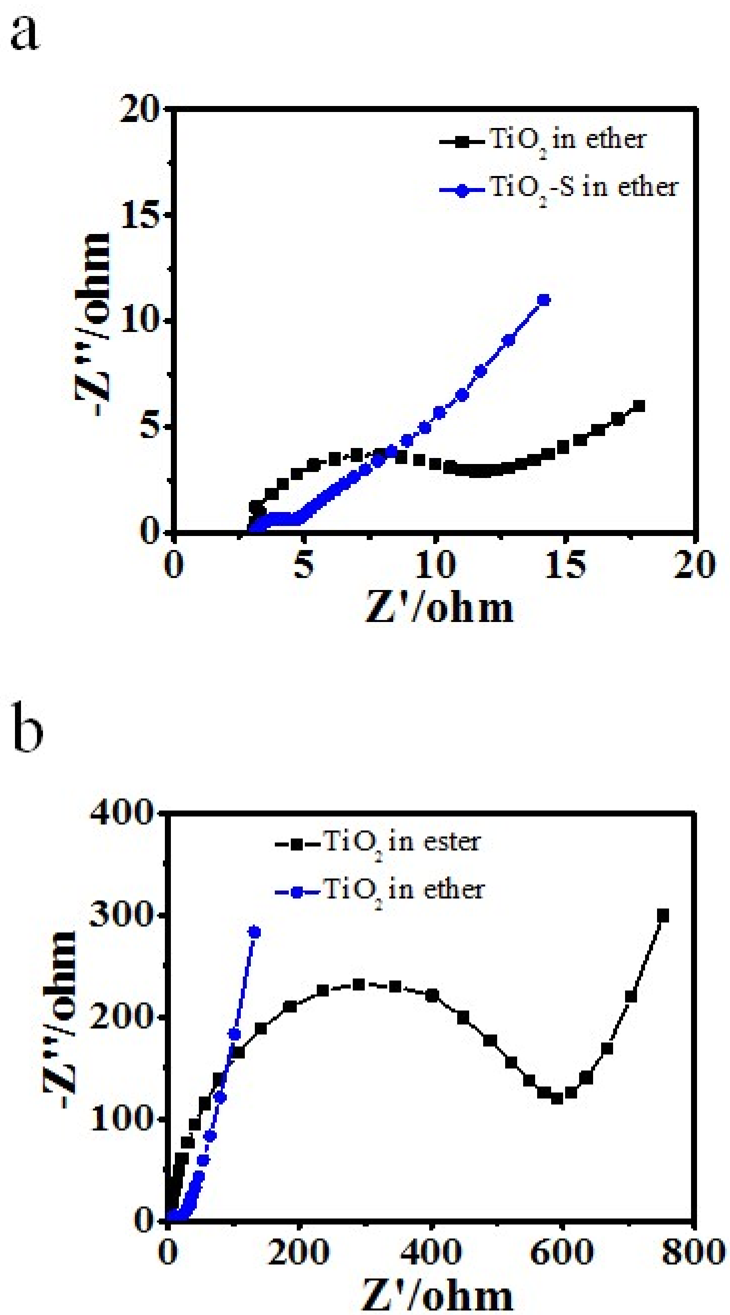

Fig. S6. EIS plots for a) different electrodes in ether and b) the TiO_2 electrode in different electrolytes.

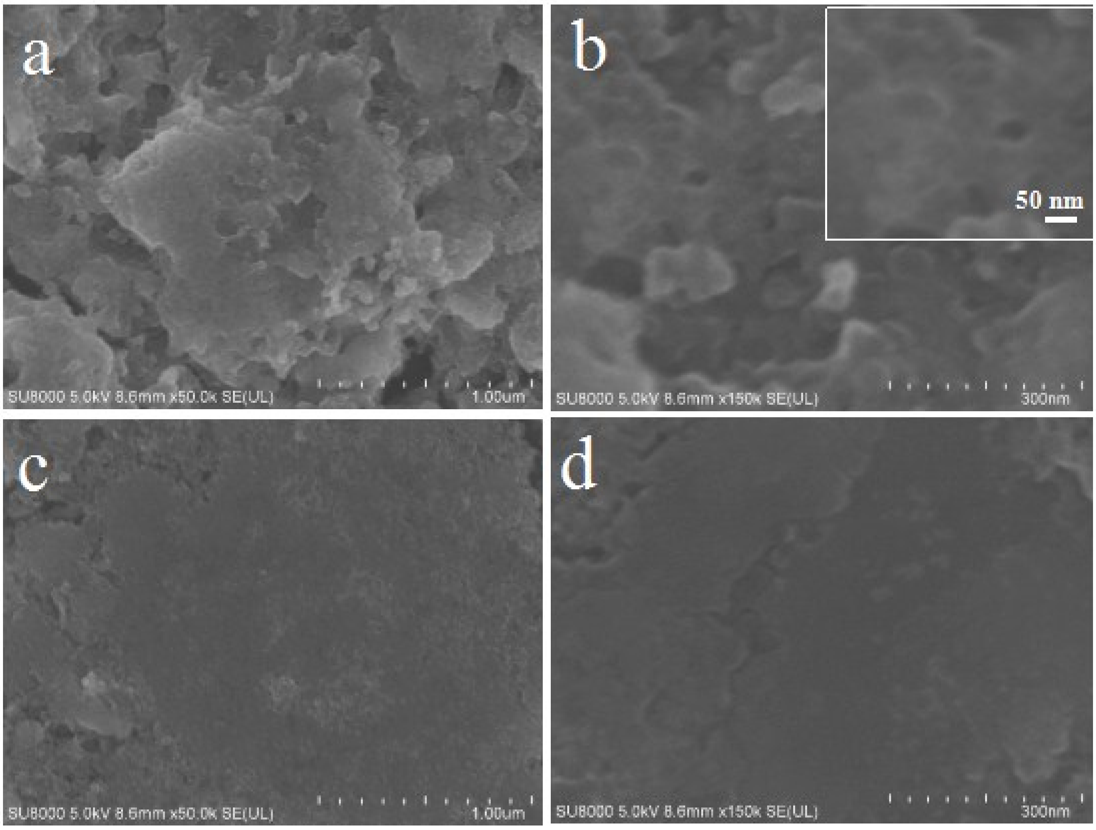

Fig. S7. SEM images for TiO_2-S electrode in (a, b) ether electrolyte and (c, d) in ester after the first discharge. The inset in b is the enlarged SEM image.

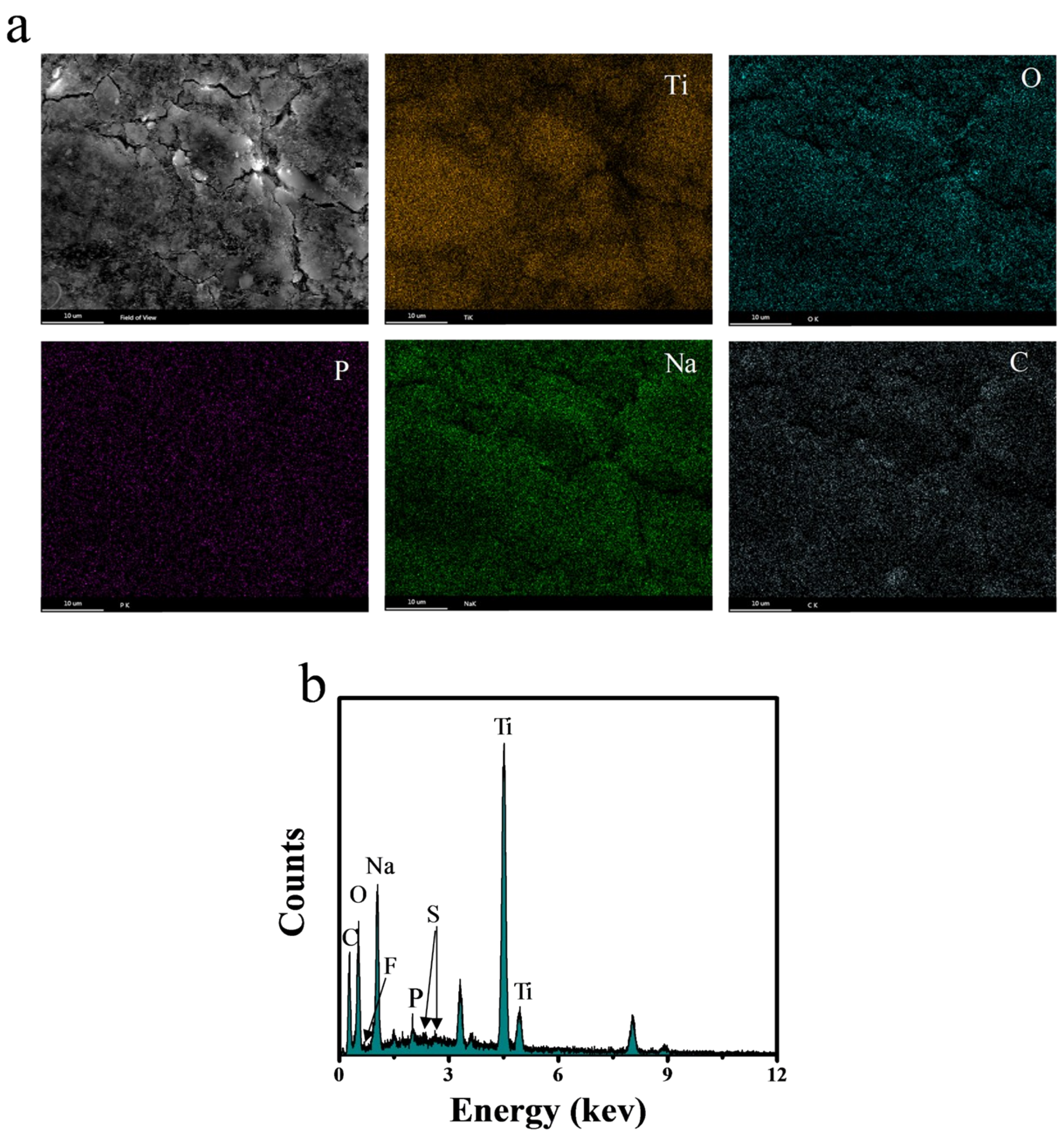

Fig. S8. The elements mapping (a) as well as correspinding full area EDS (b) of TiO_2-S electrodes after first discharge in ester.

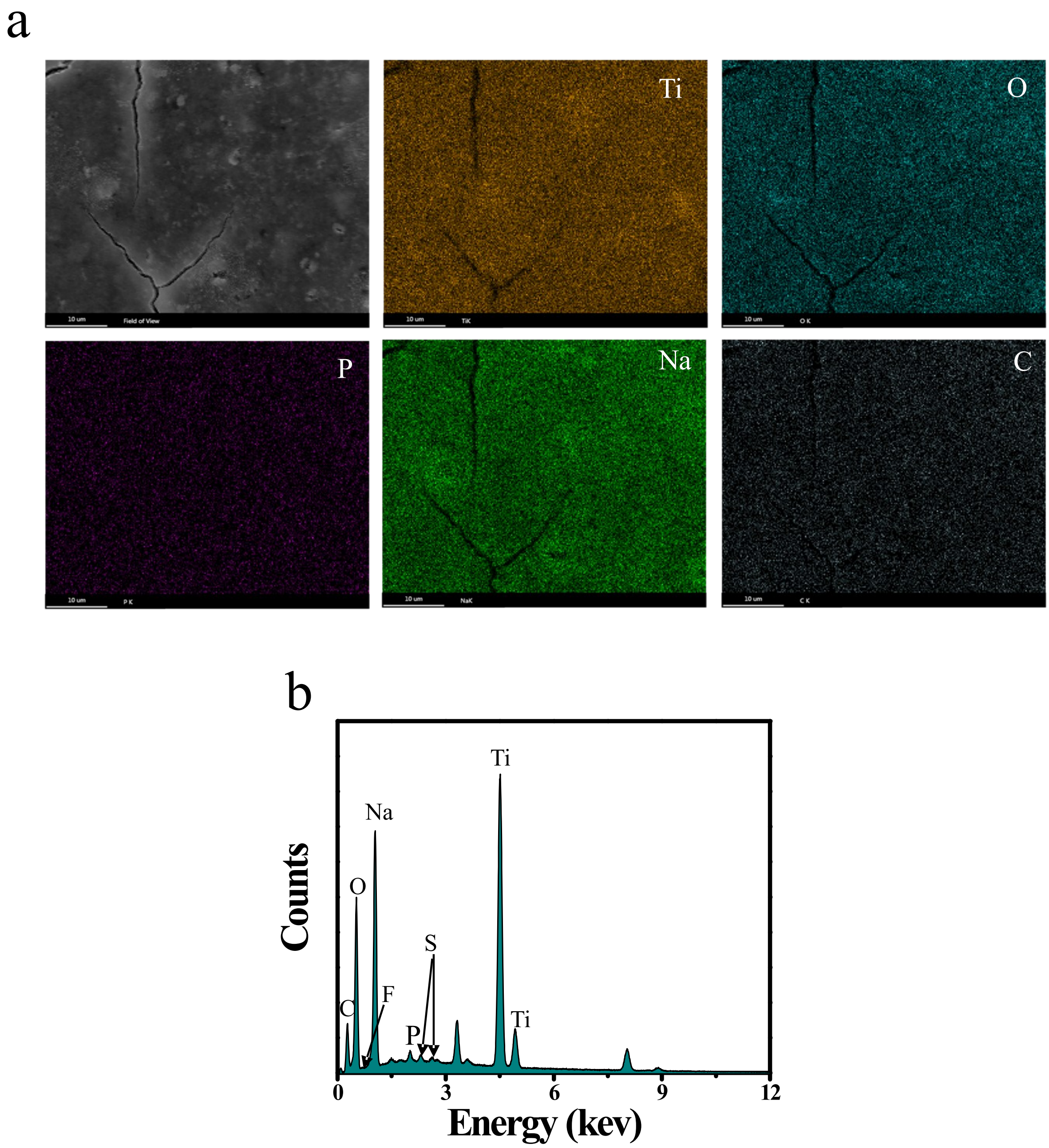

Fig. S9. The elements mapping (a) as well as correspinding full area EDS (b) of TiO_2-S electrodes after first discharge in ether.

Table S1 The various element mass percent in titanium dioxide nanosheets with sulfur doing in ester electrodes after first discharge.

Element	Ti	O	C	Na	F	P	S
Ether (%)	10.1	47.03	20.37	20.9	1.16	0.29	0.16
Ester (%)	10.22	37.99	35.12	14.07	2.01	0.41	0.18

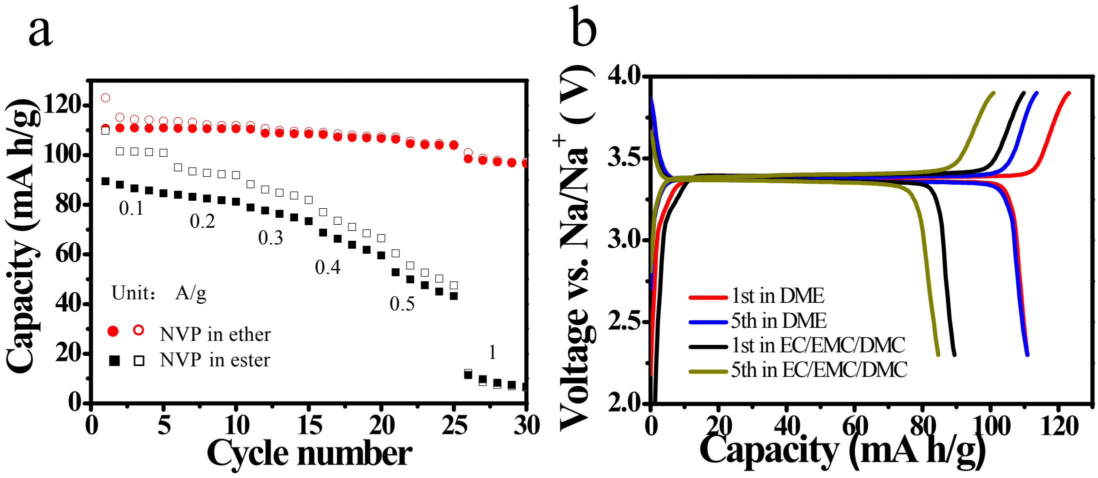

Fig. S10. The electrochemical performance of NVP cathode evaluated by half-cells within different electrolytes: a) rate capability combining with b) charge/discharge profiles at the selective cycles at 0.1 A/g.

Table S2 Comparison of representative electrochemical energy storage devices.

Anode//Cathode	Potential range (V)	Energy density (Wh/kg)	Power density (W/kg)	Cycling life	Reference
V_2O_5-CNT//AC	0-2.8	38	140	≈80% at 60C after 900 cycles	
MWTOG//AC	0.01-3	25.8	1357	≈90% at 10C after 10000 cycles	
$Na_3V_2(PO_4)_3$@C//AC	0-3	118	96	≈95% at 1.1 mA cm^{-2} after 10 000 cycles	1
$Na_2Ti_9O_{19}$ //PC	0-2.5	54	687	≈75% at 2 A g^{-1} after 2000 cycles	2
Nb_2O_5@C/rGO//AC	1–4.3	76	80	≈100% at 1 A g^{-1} after 3000 cycles	3
SCN-A//SCN-A	0-4	112	67	≈85% at 5 A g^{-1} after 3000 cycles	4
Na-TNTs//AC	0-3	34	889	≈90% at 0.25 A g^{-1} after 1000 cycles	5
$NaTi_2O_4(OH)_2$//PC	0-3	65	500	≈93% at 1 A g^{-1} after 3000 cycles	6
Nb_2O_5//PSC	1-3	43.2	5760	≈80% at 1.2 A g^{-1} after 3000 cycles	7
N-TiO_2//AC	1-4	80.3	500	≈80% at 1 A g^{-1} after 6500 cycles	
TiO_2-S//Na_2V_3(PO4)$_3$	**0.01-3.5**	**158**	**1075**	≈83% at 1 A g^{-1} after 1000 cycles	**this work**

REFERENCES

1 R. Thangavel, K. Kaliyappan, K. Kang, X. Sun and Y. S. Lee, *Adv. Energy Mater.*, 2016, **6**, 1–9.

2 S. S. M. Bhat, B. Babu, M. Feygenson, J. C. Neuefeind and M. M. Shaijumon, *ACS Appl. Mater. Interfaces*, 2018, **10**, 437–447.

3 E. Lim, J. Changshin, M. S. Kim, M. H. Kim, J. Chun, H. Kim, J. Park, K. C. Roh, K. Kang, S. Yoon and J. Lee, *Adv. Funct. Mater.*, 2016, **26**, 3711–3719.

4 H. Wang, D. Mitlin, J. Ding, Z. Li and K. Cui, *J. Mater. Chem. A*, 2016, **4**, 5149–5158.

5 J. Yin, L. Qi and H. Wang, *ACS Appl. Mater. Interfaces*, 2012, **4**, 2762–2768.

6 B. Babu and M. M. Shaijumon, *J. Power Sources*, 2017, **353**, 85–94.

7 H. Li, Y. Zhu, S. Dong, L. Shen, Z. Chen, X. Zhang and G. Yu, *Chem. Mater.*, 2016, **28**, 5753–5760.